PII: S0032-3861(96)00984-6

Polymer Vol. 38 No. 16, pp. 4019–4031, 1997
© 1997 Elsevier Science Ltd
Printed in Great Britain. All rights reserved
0032-3861/97/$17.00 + 0.00

Infrared analysis of the photochemical behaviour of segmented polyurethanes:
1. Aliphatic poly(ester-urethane)

Catherine Wilhelm and Jean-Luc Gardette*
Laboratoire de Photochimie Moléculaire et Macromoléculaire URA CNRS 433, Université Blaise Pascal et ENS de Chimie de Clermont-Ferrand, F-63177 Aubière Cedex, France
(Received 31 October 1996)

The photochemical behaviour of aliphatic-based poly(ester-urethanes) is investigated. Polymer samples are submitted to irradiation in the presence of oxygen in conditions of long wavelength irradiation ($\lambda > 300$ nm) or short wavelength irradiation ($\lambda = 254$ nm). The evolution of the structure of photooxidized polymers is monitored by *FT*i.r. analysis of thin samples and the different photoproducts formed are identified. It is shown that long wavelength irradiations provoke an induced oxidation of urethane functions. This reaction is initiated by hydrogen atom abstraction on the methylene groups in the α position of nitrogen atoms. On irradiation at short wavelength, the results provide evidence for a dual mechanism for photooxidation: induced oxidation and direct photolysis of the urethane groups following three possible photoscissions that involve the homolysis of C–N and C–O bonds. © 1997 Elsevier Science Ltd.

(Keywords: photooxidation; polyurethanes; *FT*i.r.; mechanisms)

INTRODUCTION

The photochemical processes responsible for the degradation and ultimate failure of polyurethanes have been extensively investigated for the last thirty years[1,2]. Mechanisms for the u.v.-induced oxidative process of polyether and polyester linkages have been proposed. It has been shown that the polyether component of poly(ether-urethane) contributes to the poor weathering properties of these materials[8,9]. This behaviour results from the high intrinsic oxidizability of the methylene in α of the ether function that leads to the formation of hydroperoxides and consequent chain scissions. Although far less oxidizable, the polyester component of poly(ester-urethane) may also undergo hydroperoxide formation by oxidation of the methylene in α of the ether function. However, the mechanism by which these units contribute to the degradation of these polymers is not fully understood.

Several mechanisms for the u.v.-induced oxidative process of urethane linkages have been proposed, although they are sometimes contradictory. Conventional polyurethanes based on aromatic diisocyanates, such as methylene 4,4′-diphenyl diisocyanate (MDI) or toluene diisocyanate (TDI), are known to undergo marked yellowing on exposure to u.v.-iradiation. The photolytic degradation of these polyurethanes has received considerable attention. It is generally agreed that the principal structural species responsible for discoloration of MDI-based polyurethanes are mono- and di-quinone-imide, shown in *Scheme 1*. The formation of products resulting from photo-Fries rearrangement and subsequent oxidative coupling has also been shown to provoke the discoloration of MDI- and TDI-based polyurethanes (*Scheme 2*)[9–11].

In order to obtain polymers resistant to light-induced discoloration and degradation, more costly aliphatic diisocyanates were substituted for MDI. Although polyurethanes based on aliphatic diisocyanates such as hexamethylene diisocyanate (HDI) also degrade on exposure to u.v. light, no discoloration was observed.

In previous investigations[8,9] we studied the photochemical behaviour of four classes of model polyurethanes based on various hard segments (aromatic or aliphatic) and on various elastomeric phases (polyether or polyester). At first we concentrated our investigations on the primary hydroperoxides formed on exposure of these polymers to long-wavelength light ($\lambda \geq 300$ nm) in the presence of oxygen[8], then we studied the mechanism by which the aromatic isocyanate-based polymers discoloured[9]. We focused our attention on the influence of irradiation wavelengths and on the effect of oxygen on the formation of the coloured photoproducts. The structure of the oxidized polymers was examined essentially by infrared and u.v.–visible spectroscopy combined with chemical titration of the hydroperoxidic groups. One of the main difficulties encountered in our investigations was the opacity of polyurethanes in the i.r. domains of interest: the NH and C=O stretching vibrations of urethane and/or ester groups result in high absorption in the hydroxyl and carbonyl domains.

Since this work was published (1981), the basic knowledge in the field of polymer photodegradation has improved. So have the analytical tools, particularly since the development of *FT*i.r. spectroscopy. It now appears possible to gain a better insight into the

---

* To whom correspondence should be addressed

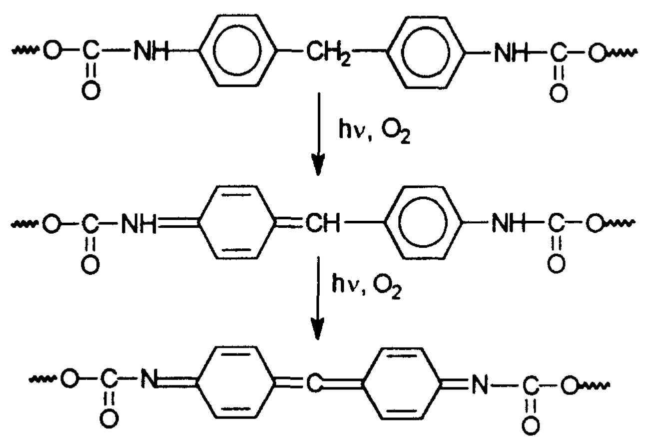

Scheme 1 Formation of mono- and di-quinone-imide in MDI-based polyurethanes

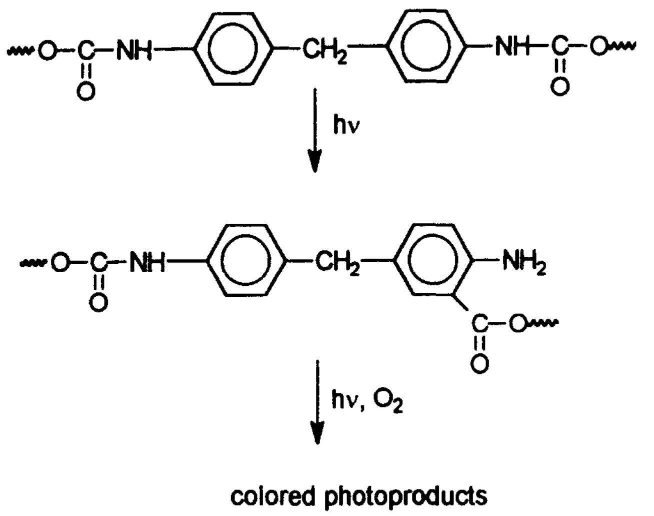

Scheme 2 Photo-Fries type mechanism in MDI-based polyurethanes

photodegradation mechanisms of polyurethanes. In a series of papers, we will report on the photochemical behaviour of four classes of model polymers based on aromatic or aliphatic diisocyanates and on polyether or polyester macrodiols.

In this paper, we describe the photochemical evolution of three model compounds based on aliphatic diisocyanate. The first model compound was obtained by polycondensation of hexamethylene diisocyanate (HDI) on 1,4-butanediol (BDO). The simple structure of this model may allow a better understanding of the reactivity of urethane linkage due to the absence of other reactive sites and to a simplified infrared spectrum as opposed to that of poly(ester-urethane). Indeed, i.r. absorption of the ester structure is strong and hides most of the hydroxylated and carbonylated photooxidation products. On the basis of the results obtained with the simplified model, we will describe the behaviour of two aliphatic polyurethanes elaborated from two polyesters having different molecular weights.

EXPERIMENTAL

Materials and synthesis

The materials used in this study were aliphatic segmented polyurethanes. Segmented polyurethanes are block polymers composed of alternating soft segments (polyester) and hard segments (urethane).

The formulae of the different products used in the synthesis of polyurethanes are listed in *Table 1*.

The model compound, HDI–BDO, which involved no soft segments, was obtained by reacting one part hexamethylene diisocyanate (HDI) with one part 1,4-butanediol (BDO). Polymerization was carried out in tetrahydrofuran (THF) solution with a total concentration of reactants of about 10%. Dibutyltindilaurate (DBTDL) (0.01 wt% of the reactants) was used as catalyst and the reaction was carried out at 50°C under N_2 for 12 h. The polymer obtained was precipitated in methanol, then filtered and dried.

The two models of block polyurethanes that include soft segments were synthesized following the standard prepolymer method[13]. The soft segments used were poly(tetramethylene ethylene adipate) (PABE), containing about 10% of ethylene structure. The average molecular weights of the polyesters used for the synthesis were respectively 560 and 2000 (PABE 560 and PABE 2000). The chain extender used was 1,4-butanediol (BDO). Taking into account the true functionality of oligomers, polycondensation of three parts HDI with one part PABE was carried out in bulk at 80°C for 4 h. Then THF was added with three parts BDO and 0.01% DBTDL at room temperature to encourage chain extension. The total concentration of polymer in THF was about 10%. The reaction proceeded at 50°C under N_2 for 15 h. The polymers were precipitated in methanol, then filtered and dried at room temperature. Those two polymers are called ESHDI 560 and ESHDI 2000.

Preparation of samples

Due to the strong infrared absorption of the urethane structure, *FT*i.r., analysis required very thin samples (5–10 μm) to be within an absorbance range where the Beer–Lambert law is obeyed.

The three models were dissolved in 1,1,1,3,3,3-hexafluoroisopropanol (HFIP). For the model compound

Table 1 Characteristics of products used for the synthesis

Diisocyanate: hexamethylenediisocyanate, HDI	$NCO{-}(CH_2)_6{-}NCO$ $M_w = 168\,g\,mol^{-1}$
Chain extender: 1,4-butanediol, BDO	$OH{-}(CH_2)_4{-}OH$ $M_w = 90\,g\,mol^{-1}$
α–ω Hydroxy-terminated oligomer: poly(tetramethylene ethylene adiphate) with 10% of ethylene, PABE	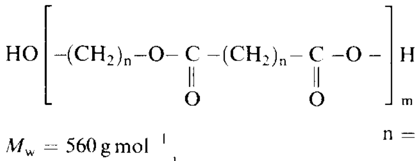 $HO\left[-(CH_2)_n{-}O{-}\underset{\displaystyle O}{\overset{}{\underset{\Vert}{C}}}{-}(CH_2)_n{-}\underset{\displaystyle O}{\underset{\Vert}{C}}{-}O{-}\right]_m H$ n = 2 or $M_w = 560\,g\,mol^{-1}$ $M_w = 2000\,g\,mol^{-1}$

ESHDI 2000, films were cast from HFIP solutions onto glass dishes. After evaporation of the solvent at room temperature, the films were fixed on sample holders used for u.v. irradiation and *FT*i.r. transmission analysis.

Irradiation and analysis

The polymer samples ESHDI and the model compound HDI–BDO were irradiated in a SEPAP 12-24 unit at 60°C. This medium-accelerated photoaging device has been described in several papers (see for instance ref. 14). It allows irradiation at wavelengths above 300 nm.

Short-wavelength irradiation ($\lambda = 253.7$ nm) was carried out in a cylindrical unit equipped with six low-pressure mercury lamps emitting mainly at 253.7 nm (described in ref. 15).

Fourier transform infrared (*FT*i.r.) spectra in transmission mode were recorded using a Nicolet 20SX spectrometer equipped with a TGS detector using 32 scans summation at a nominal resolution of 2 cm^{-1}.

For photolysis experiments, polymer samples were placed in Pyrex tubes (for long-wavelength irradiation) or quartz tubes (for short-wavelength irradiation) and sealed under vacuum (10^{-6} torr) obtained using a mercury diffusion vacuum line.

Photooxidized films were exposed to reactive gases at room temperature in a simple flow system that could be sealed off to allow the reaction to proceed. The gases used for chemical derivatization reactions were SF_4 and NH_3 (supplied respectively by Fluka and UCAR). SF_4 treatments were carried out in an all-Teflon system because SF_4 attacks glass.

RESULTS

Interpretation of the initial i.r. spectra

Since the experimental results reported here were based on the analysis of the evolution of i.r. spectra of photooxidized polyurethanes, the absorption frequencies of the polymers under investigation had first to be precisely assigned.

In order to assign the different maxima observed on the i.r. spectra of the three models (HDI–BDO, ESHDI 560 and ESHDI 2000), we had to compare these models with each other and with the compounds used for their synthesis (HDI, PABE), and with low molecular weight compounds of similar structure (ethyl N-ethyl carbamate and ethyl carbamate)[16]. The assignments are given in *Tables 2* and *3*.

Long-wavelength ($\lambda > 300$ nm) irradiation

In absence of oxygen. The i.r. spectra of the three model compounds were recorded for long-wavelength irradiation carried out in the absence of oxygen. No noticeable evolution of the spectra was observed, even for prolonged irradiation times.

In presence of oxygen. (a) Photooxidation of the model compound HDI–BDO. The photooxidation of HDI–BDO caused severe modifications to the i.r. spectra of the irradiated samples.

The changes in the i.r. spectra are shown in *Figures 1–3* in relation to different zones of the spectra and corresponding to irradiation times of up to 960 h. This evolution corresponds to a low extent of oxidation and as a consequence the modifications remain low. The direct

Table 2 Absorption band assignments for HDI–BDO

Frequency (cm^{-1})[a]	Relative intensity[b]	Main assignments[c]	References
3420	vw, sh	υ (NH) free	4, 17
3320	vs	υ (NH) bonded	8, 11, 17, 19
3054	w	overtone of amide II band	
2960	sh	υ_{as} (CH_2) in BDO	17
2940	vs	υ_{as} (CH_2) in HDI	21
2871	m	υ_{sym} (CH_2) in BDO	17
2860	m	υ_{sym} (CH_2) in HDI	21
1720	vw, sh	υ (C=O) free	19, 20
1688	vs	υ (C=O) bonded	19, 20
1540	s	δ (NH) + υ (CN) amide II band	17, 20
1478	w	δ (CH_2)	
1466	vw	δ (CH_2)	
1458	vw	δ (CH_2)	
1337	m	δ (CH_2) in HDI or ω (CH_2)	17
1263	vs	υ (CN) + δ (NH) amide III band	
1244	w, sh	υ (C=O) + υ (O–CH_2)	
1222	m	υ (C–O–C)	2
1140	s	υ (C=O) + υ (O–CH_2)	17
1065	m	υ (C–O–C)	2
1048	sh, w	υ (C–N)	
997	m	υ (C–C) in HDI	
772	s	β (CH_2) or γ (CO–O–C)	17
751	w	β (CH_2)	2
733	m	β (CH_2)	
638	s	ω (NH) amide V band	
587	sh	β (CH_2)	

[a] In the infrared analysis, absorption frequencies are accurate to 2 cm^{-1}
[b] The relative intensity is based on the whole infrared spectrum of a sample at room temperature: w = weak, m = medium, s = strong, vs = strong, sh = shoulder
[c] The main assignments are: υ = stretching, δ = bending, ω = wagging, β = in plane bending, υ_{as} = assymetric stretching, υ_{sym} = symmetric stretching

Table 3 Absorption band assignments for the soft PABE segment

Frequency (cm^{-1})[a]	Relative intensity[b]	Main assignments[c]	References
~3550	vw	overtone of υ (C=O)	
3450	vw		
2958	s	υ $(CH_2)_{ass}$	17
2922	vw, sh	υ $(CH_2)_{ass}$	17
2900	vw, sh	υ $(CH_2)_{sym}$	17
2874	w	υ $(CH_2)_{sym}$	
1735	vs	υ (C=O)	2, 17
1490	vw	δ (CH_2)	17
1476	vw	δ (CH_2)	17
1465	vw	δ (CH_2)	17,18
1414	vw	δ (CH_2)	
1403	vw	δ (CH_2)	
1371	vw	δ (CH_2)	
1233	w, sh	υ (C=O) + υ(O–CH_2) O	
1180	s	υ (C–O–C)–C–O–C	17, 2, 22
1140	s	υ (C=O) + υ (O–CH_2)	
1067	m	υ(C–O–C) $-\overset{\overset{O}{\Vert}}{C}\ -O\overset{\downarrow}{-}C$	2
960	vw		
931	vw		
912	vw		
736	w	β (CH_2)	2
586	vw	β (CH_2)	

[a] In the infrared analysis, absorption frequencies are accurate to 2 cm^{-1}
[b] The relative intensity is based on the whole infrared spectrum of a sample at room temperature: w = weak, m = medium, s = strong, vs = very strong, sh = shoulder
[c] The main assignments are: υ = stretching, δ = bending, ω = wagging, β = in plane bending, υ_{as} = asymmetric stretching, υ_{sym} = symmetric stretching

spectra and the subtraction of the initial spectrum from the spectra recorded after several irradiation times permits us to characterize this evolution in the different domains.

In the hydroxyl domain (*Figure 1*) a broad band increased between 3600 and 3050 cm^{-1} which indicated the formation of hydroxyl structures along with evolution of the NH absorptions. The increase of a broad complex carbonyl band was observed, overlaying the decrease of the v (C=O) bands of the urethane group (*Figure 2*).

A substantial loss of urethane structures was indicated by the decrease in the intensity of the bands at 3320 cm^{-1} (amide II), 1263 cm^{-1} (amide III), 781 cm^{-1} (δ(N–H)) and 638 cm^{-1} (amide V).

An appreciable decline of the absorption bands at 2940 and 2860 cm^{-1} (respectively v_{ass} (C–H) and v_{sym} (C–H)) and at 1478, 1466 and 1458 cm^{-1} (δ(CH$_2$)) indicated a loss in the methylene group content in α position to the NH. The bands assigned to the

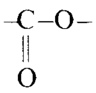

$$-\underset{\displaystyle O}{\underset{\|}{C}}-O-$$

groups of the carbamate structures at 1244 and 1140 cm^{-1} were also observed to decrease substantially (*Figure 3*).

A broadening of the 3320 cm^{-1} band was observed. Despite poor resolution, the evolution suggested the appearance of absorption maxima at 3180 and 3450 cm^{-1}, which accounts for the formation of hydroxylated photoproducts.

In the carbonyl domain, the urethane carbonyl band (1688–1720 cm^{-1}) gradually broadened with increasing irradiation time, leading to the formation of a shoulder at higher frequencies (1800-1700 cm^{-1}). The differences between spectra on *Figure 2* permit us to characterize this shoulder by four maxima at 1785, 1755, 1737 and 1715 cm^{-1}. It may be postulated that more maxima were increasing at lower frequencies (around 1700 cm^{-1}), but they developed concurrently with the decrease of the initial urethane carbonyl band and as a consequence could not be observed distinctly on the spectra.

On the same figure, it is observed that a weak band at 1607 cm^{-1} increased when the near band at 1540 cm^{-1} decreased. The shape of this evolution strongly suggested that the decrease of the 1540 cm^{-1} band had to be related to the increase of the 1607 cm^{-1} band.

In the domain of the deformation vibrations, one may observe the formation of several bands at 1495, 1410, 1340, 1204, 1170 and 1078 cm^{-1} (*Figure 3*).

In the domain 900–400 cm^{-1}, despite poor resolution due to the weak intensity of the initial bands, one may observe a decline of the bands at 772 and 638 cm^{-1}.

In presence of oxygen. (b) Photooxidation of ESHDI 560 and ESHDI 2000: influence of the polyester segments. In this section, results are presented for the influence of the soft segments on the photooxidation of the two segmented polyurethanes: ESHDI 560 and ESHDI 2000.

First, it should be noted that the i.r. spectral evolutions of these two model compounds under u.v. irradiation were similar to those reported above in the case of HDI–BDO. The differences of spectra, compared to the previous band attributions, showed that the decrease of absorption bands corresponded to urethane groups. No

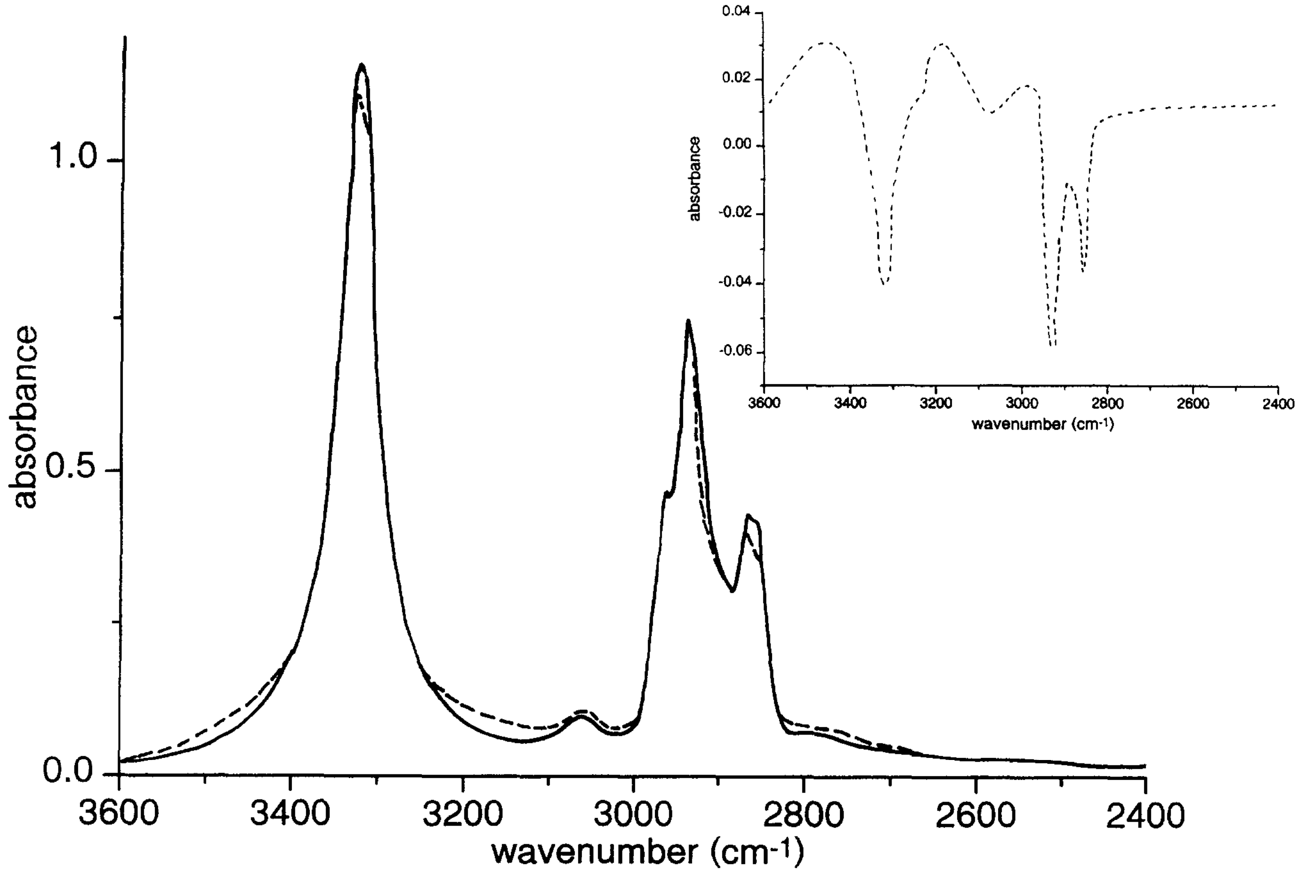

Figure 1 Evolution of the spectrum of the HDI–BDO model on irradiation at long wavelength: —— initial; – – – 960 h. The insert shows the initial spectrum subtracted from the spectrum of the photooxidized film

decrease of the i.r. bands assigned to the ester function was observed.

It appeared then that no influence of the ester functions on the photochemical behaviour of either polymer could be identified for long-wavelength irradiation. The non-reactivity of the ester component of these polyurethanes was confirmed by the fact that, on irradiation under the same experimental conditions, no evolution of the i.r. spectra of poly(tetramethylene ethylene) adipate was observed, even for longer exposure times.

In conclusion, it should be pointed out that for long-wavelength irradiation no influence of the polyester soft segments on the photochemical behaviour of aliphatic poly(ester-urethane) was observed. The evolution of the i.r. spectra of irradiated poly(ester-urethane) may then be interpreted from those of HDI–BDO.

Chemical treatments of photooxidized samples. Derivatization reactions have been used to identify the oxidation photoproducts observed by i.r. analysis. These reactions were carried out by treating photooxidized samples with gaseous reactants (sulfur tetrafluoride, ammonia).

Carboxylic acids react with SF_4 to give 1,1,1-trifluorides[23]. The first product of this reaction is an acyl fluoride than can be isolated:

$$RCOOH + SF_4 \rightarrow RCOF$$

The reactions with carboxylic acids to give acyl fluorides and with alcohols or hydroperoxides to give alkyl fluorides are those most likely to occur.

Acyl fluorides formed by reaction of carboxylic acid with SF_4 are characterized by a distinct C=O absorption above $1800\,\mathrm{cm}^{-1}$[24]. Treatment by SF_4 carried out on a photooxidized ESHDI sample as well as on a photooxidized HDI–BDO sample gave an absorption band at $1841\,\mathrm{cm}^{-1}$ (*Figure 4*).

Although some data on the i.r. absorption of acyl fluorides were available in the literature[24], they concerned compounds in solution and some former results have shown that matrix effects could be suspected. To obtain accurate assignments, the matrix effect on the C=O frequencies of different acyl fluorides formed in different polymers was studied. The results obtained are detailed elsewhere[25]. For example, hexanoic acid, introduced in an ESHDI 2000 film and then subjected to SF_4, gave a new C=O absorption band at $1841\,\mathrm{cm}^{-1}$.

The reaction of ammonia with an ESHDI sample led to a decrease of the carbonyl bands between $1750\,\mathrm{cm}^{-1}$ and $1700\,\mathrm{cm}^{-1}$ and to an increase of absorbance between 1500 and $1630\,\mathrm{cm}^{-1}$ with a maximum around $1560\,\mathrm{cm}^{-1}$.

Carboxylic acids react with NH_3 to give carboxylate ions:

$$ROOOH + NH_3 \rightarrow RCOO^-, NH_4^+$$

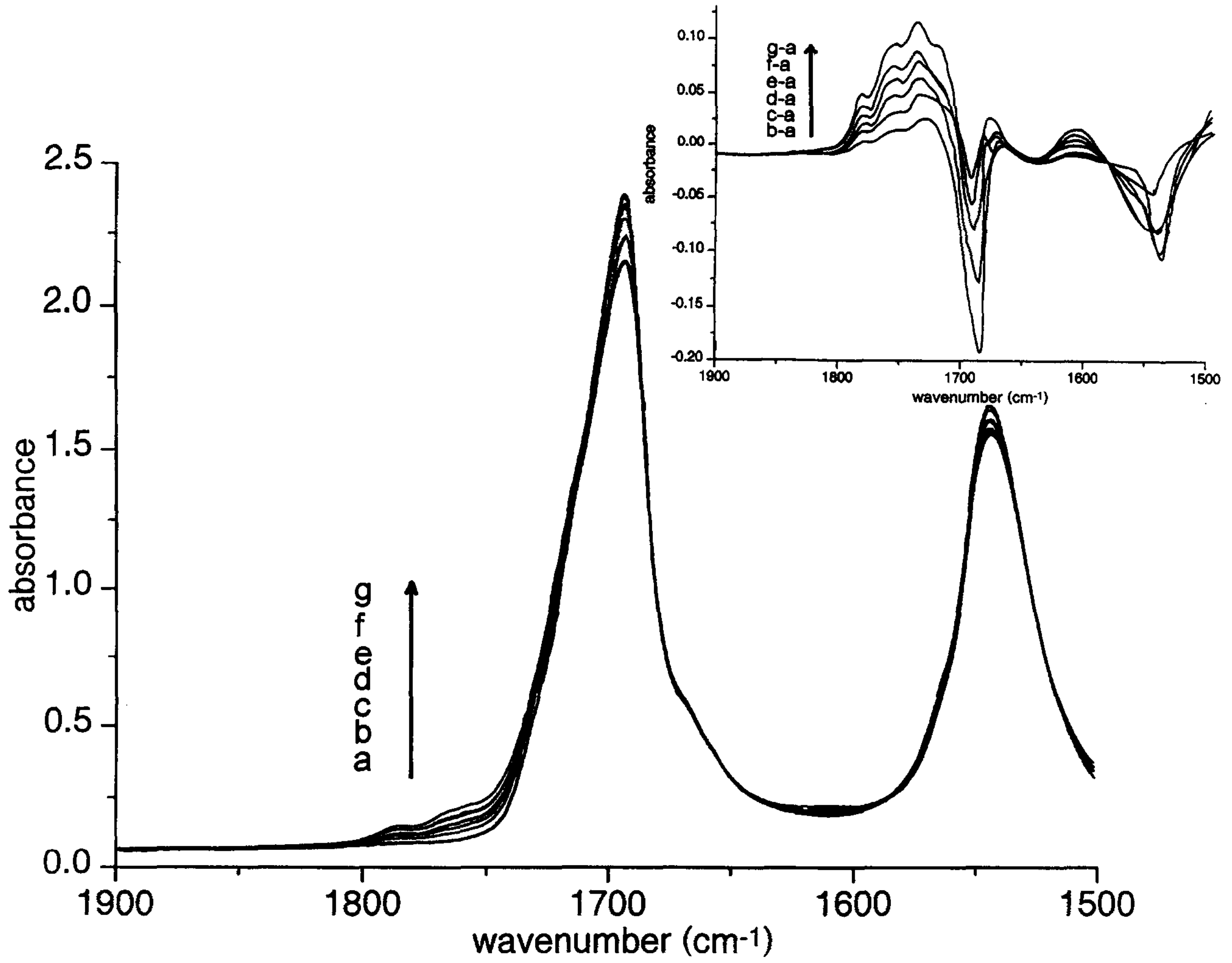

Figure 2 Evolution of the spectrum of the HDI–BDO model on irradiation at long wavelength for 960 h: a: 0 h; b: 100 h; c: 320 h; d: 455 h; e: 604 h; f: 774 h; g: 960 h. The insert shows the initial spectrum subtracted from the spectrum of the photooxidized film

Carboxylate ions derived from aliphatic acids usually present an absorption maximum around 1560 cm^{-1}.

Short-wavelength photooxidation ($\lambda = 254$ nm)

Influence of the soft segment. Samples of HDI–BDO and ESHDI 560 or 2000 were irradiated in the presence of atmospheric oxygen under monochromatic light ($\lambda = 254$ nm).

In contrast to the results presented above for long-wavelength conditions, irradiation at short wavelength gave quite similar evolutions for the HDI–BDO and ESHDI models except for an important decrease of the bands assigned to the ester functions. For HDI–BDO, the main difference from the evolution reported above for long-wavelength irradiation are as follows:

- In the spectral domain 3600–2400 cm^{-1}, there was observed the growth of an intense broad band with a shoulder at 3205 cm^{-1} (*Figure 5*). The subtracted spectra showed the decrease of the bands at 2940 and 2858 cm^{-1} (respectively υ_{asym} (C–H) and υ_{sym}(C–H)) and of two bands at 2871 and 2858 cm^{-1} (respectively υ_{asym} (C–H) and υ_{sym} (C–H)) that correspond to the stretching vibrations of both methylenes in α position to the urethane groups:

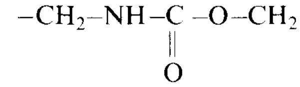

$$-CH_2-NH-\underset{\underset{O}{\|}}{C}-O-CH_2-$$

- In the domain 1900–1500 cm^{-1}, the maximum at 1755 cm^{-1} reported above was not observed. Only a broadening of the initial band was recorded, with a shoulder at 1785 cm^{-1}, and the decrease of the urethane band at 1688 cm^{-1} prevented observation of any definite maximum between 1720 and 1670 cm^{-1} (*Figures 6a* and *b*).
- In the domain 1500–900 cm^{-1}, no maximum at 1204 cm^{-1} was observed, but a substantial growth of a band at 1025 cm^{-1} was observed.

As for the ESHDI models, in addition to the changes reported for HDI–BDO, there was observed a marked decrease of the absorption bands assigned to the polyester component (*Figures 7a* and *b*). This behaviour indicates a decarboxylation of the ester groups.

Photooxidation of poly(tetramethylene ethylene adipate). Under the same irradiation conditions, the changes in the i.r. spectrum of poly(tetramethylene ethylene adipate) were characterized by an appreciable loss of ester structure, as indicated by the decline of the bands at 1731, 1263, 1167 and 1065 cm^{-1}. A weak increase of absorption was observed in the hydroxyl domain with a maximum at 3223 cm^{-1} and in the carbonyl domain by a broad band with a shoulder at 1778 cm^{-1}. The decline of the ester band at 1731 cm^{-1}, however, prevented observation of the absorption maximum of the broad band.

DISCUSSION

It is not the aim of the paper to discuss the nature and chemical structure of the chromophors that induce the oxidation of the polymer matrix. This general problem of the induced oxidation of non-absorbing polymers has

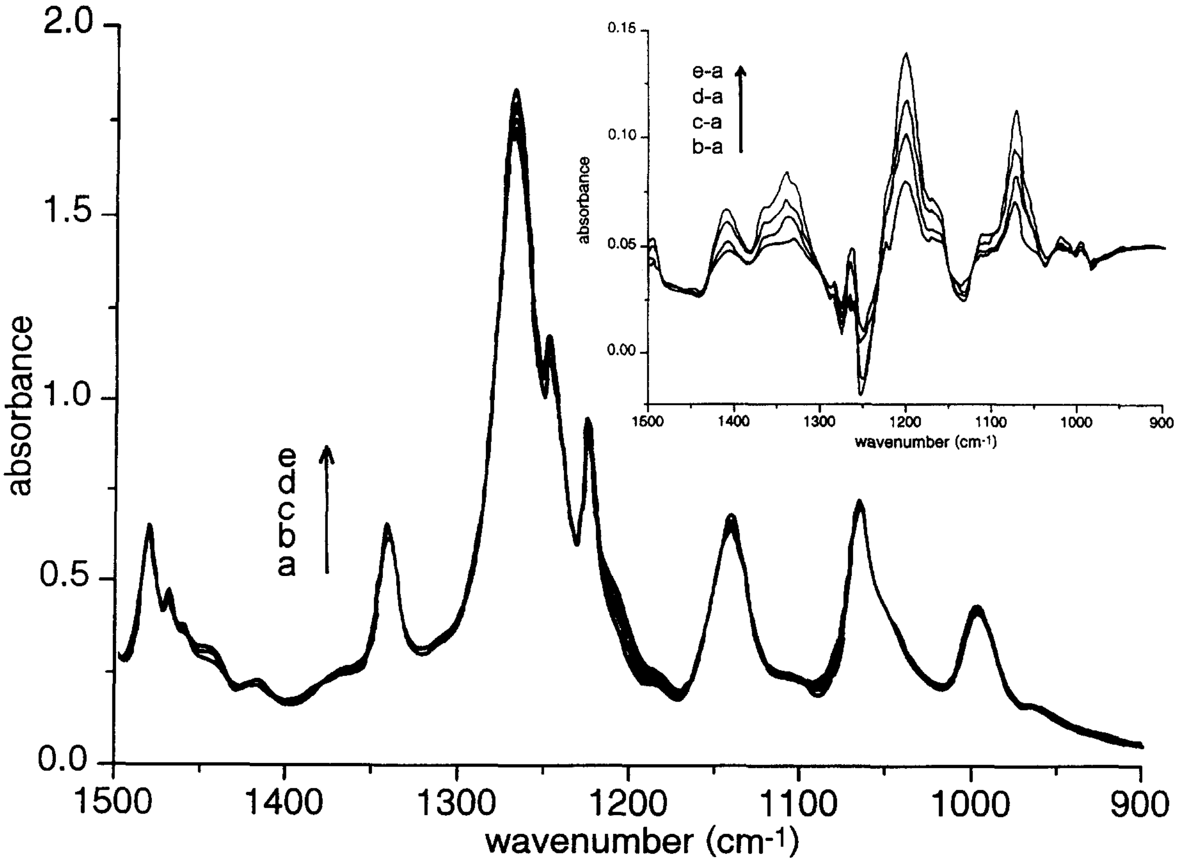

Figure 3 Evolution of the spectrum of the HDI–BDO model on irradiation at long wavelength for 960 h: a: 0 h; b: 320 h; c: 455 h; d: 604 h; e: 960 h. The insert shows the initial spectrum subtracted from the spectrum of the photooxidized film

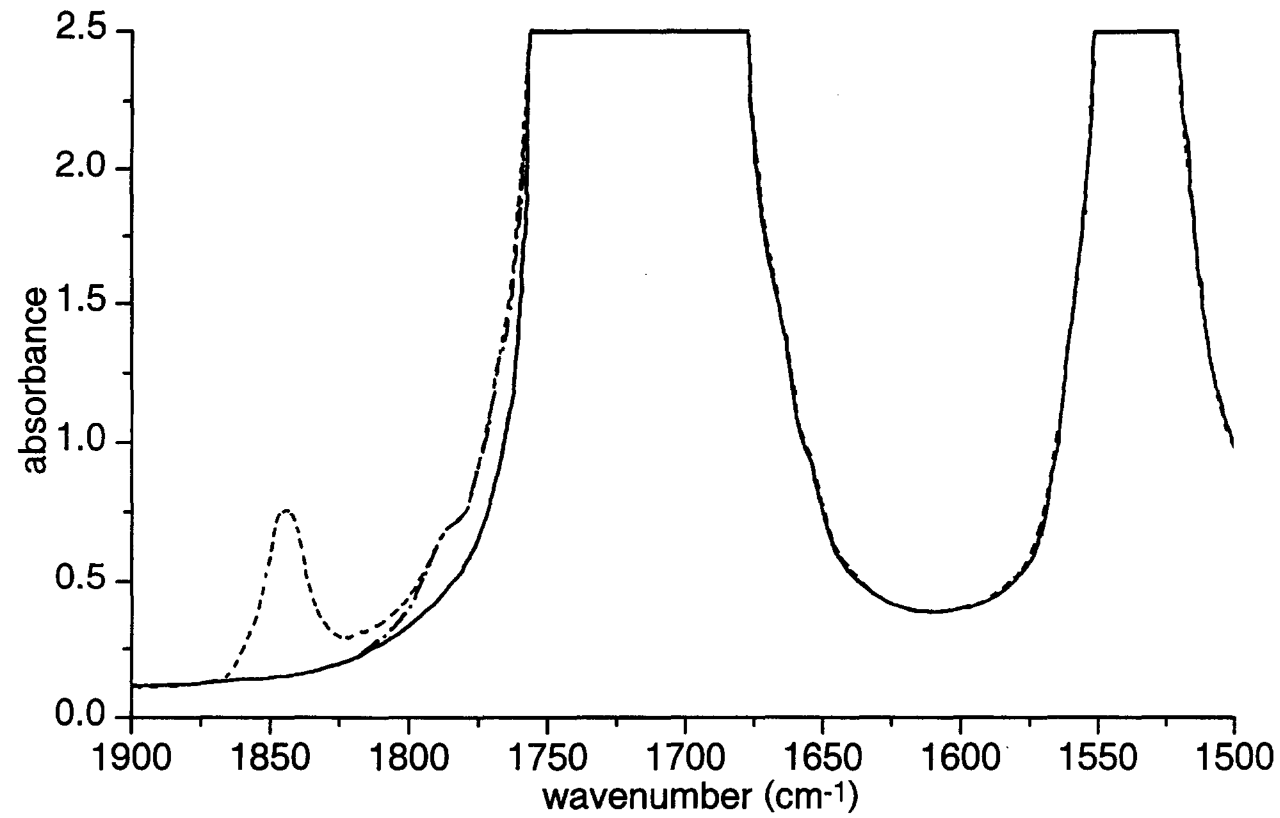

Figure 4 Effect of SF$_4$ treatment on an ESHDI 2000 model after photooxidation: —— initial; - - - after 960 h of irradiation; — — — after SF$_4$ reaction

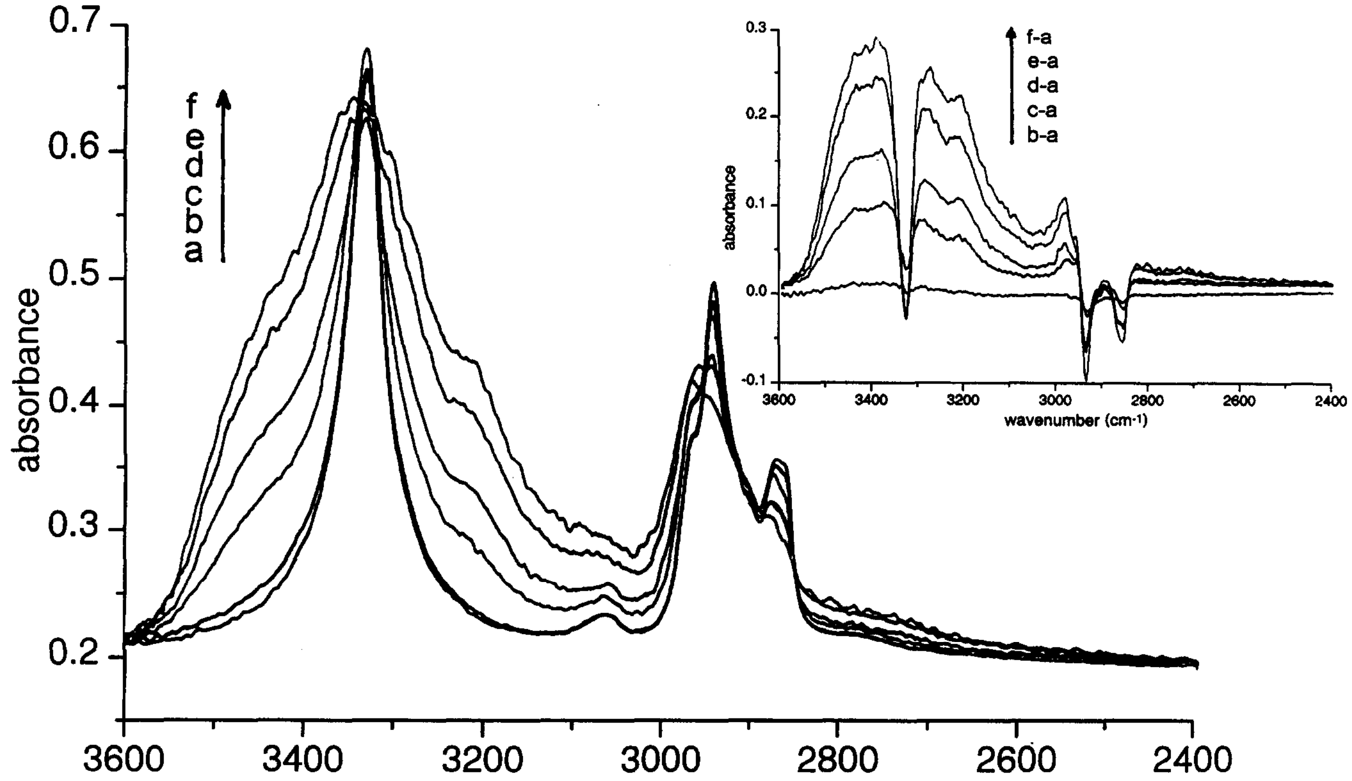

Figure 5 Evolution of the spectrum of the HDI–BDO model on irradiation at short wavelength for 960 h: a: 0 h; b: 123 h; c: 406 h; d: 572 h; e: 742 h; f: 930 h. The insert shows the initial spectrum subtracted from the spectra of the photooxidized films

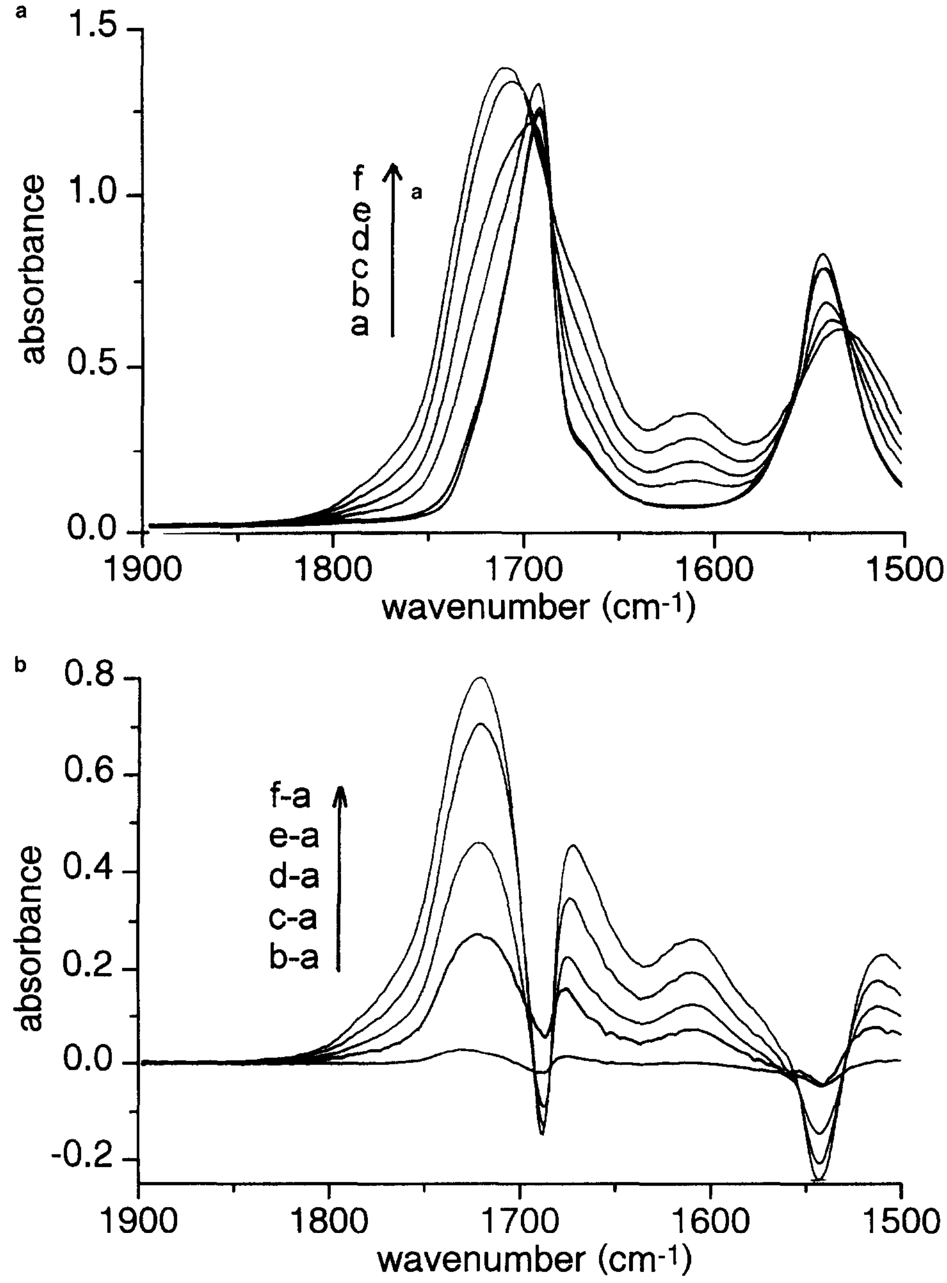

Figure 6 (a) Evolution of the spectrum of the HDI–BDO model on irradiation at short wavelength ($\lambda = 254$ nm): a: 0 h; b: 123 h; c: 406 h; d: 572 h; e: 742 h; f: 930 h. (b) Subtraction of the initial spectrum from the spectrum of the photooxidized film

been reviewed many times and it is well agreed that, among the many possible candidates, extrinsic chromophores formed during the synthesis and preparation of the samples are the most probable ones to induce the oxidation of the polymer matrix.

In conditions of irradiation at long wavelengths, no difference of behaviour was observed for the three compounds, which showed that, in these conditions of irradiation, the polyester component has little reactivity in comparison to the reactivity of polytetra(methylene ethylene adipate). This result shows that only the reactivity of the urethane function

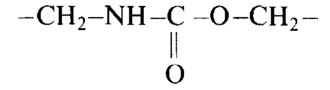

$$-CH_2-NH-\underset{\underset{O}{\parallel}}{C}-O-CH_2-$$

is involved.

For long wavelength irradiation, a selective loss in the intensity of methylene groups at 2940 and 2860 cm^{-1} was observed, which indicates an oxidation of the carbon atom in α position to the NH of urethane groups. This radical-induced oxidation leads to the formation of primary hydroperoxides:

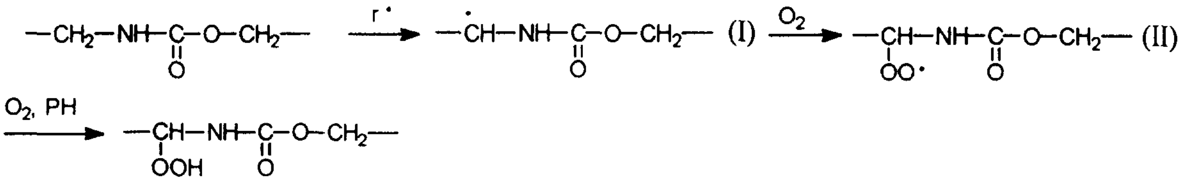

$$-CH_2-NH-\underset{\underset{O}{\parallel}}{C}-O-CH_2- \xrightarrow{r^\bullet} -\overset{\bullet}{C}H-NH-\underset{\underset{O}{\parallel}}{C}-O-CH_2- \text{ (I)} \xrightarrow{O_2} -\underset{\underset{OO^\bullet}{|}}{C}H-NH-\underset{\underset{O}{\parallel}}{C}-O-CH_2- \text{ (II)}$$

$$\xrightarrow{O_2,\ PH} -\underset{\underset{OOH}{|}}{C}H-NH-\underset{\underset{O}{\parallel}}{C}-O-CH_2-$$

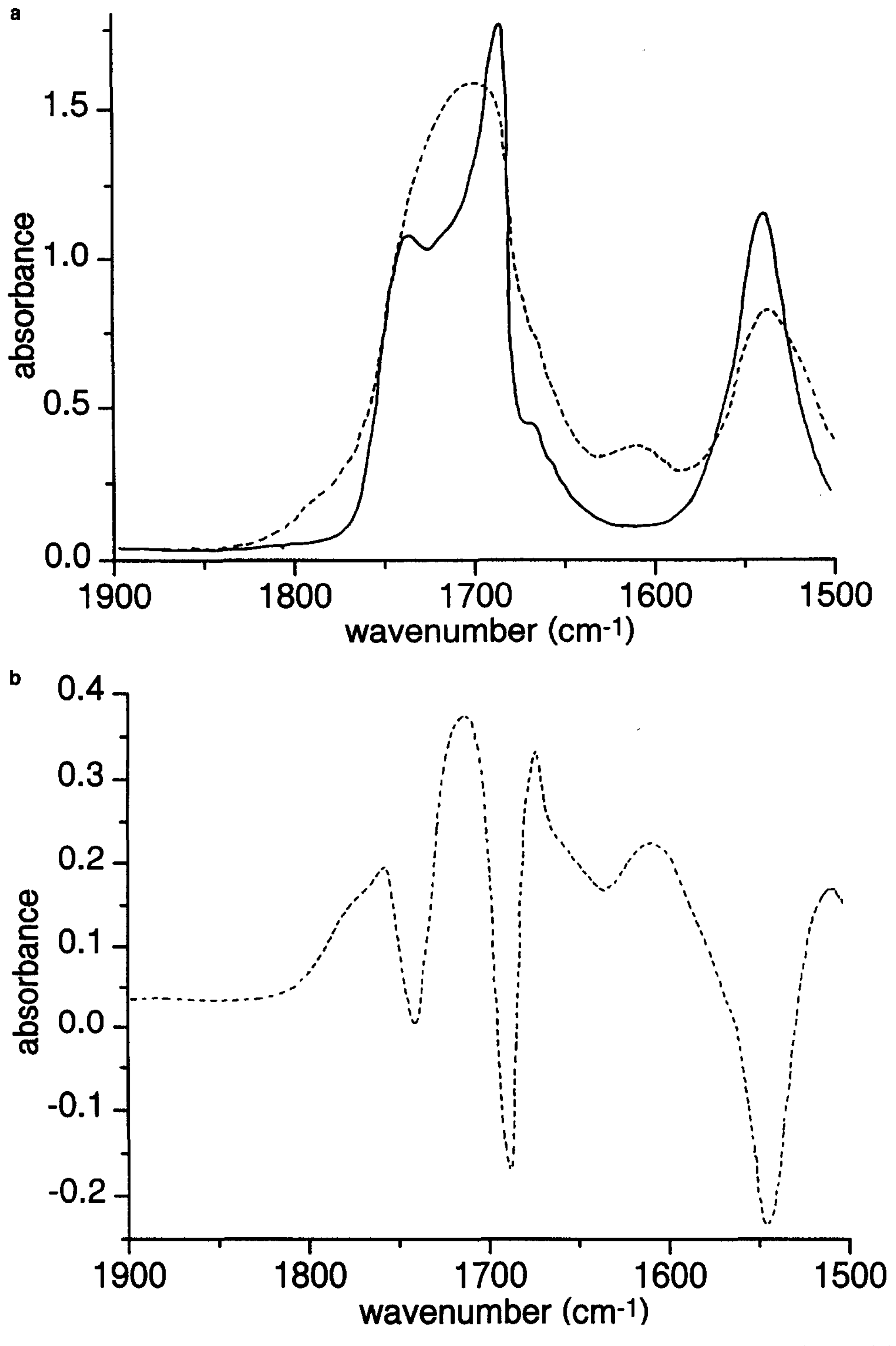

Figure 7 (a) Evolution of the spectrum of the ESHDI 560 model on irradiation at short wavelength ($\lambda = 254$ nm): —— initial; - - - 500 h. (b) Subtraction of the initial spectrum from the spectrum of the photooxidized film

The reactivity of α-methylene has been shown previously by Beachell and Chang[1]. The authors have shown that the u.v. irradiation of ethyl N-ethyl carbamate led to the formation of the radical CH_3–CH–CO–O–C_2H_5. The primary hydroperoxides formed by oxidation of methylene groups had been detected and chemically titrated in a previous study of the photooxidation of ESHDI 2000. The hydroperoxides accumulate up to low stationary concentrations around 60 mmol kg^{-1} [8]. They can decompose thermally or photochemically to give a macroalcoxyradical (III) and a hydroxyl radical HO•. The main route of evolution of this pair of radicals involves a cage reaction that leads to the formation of an acetylurethane function:

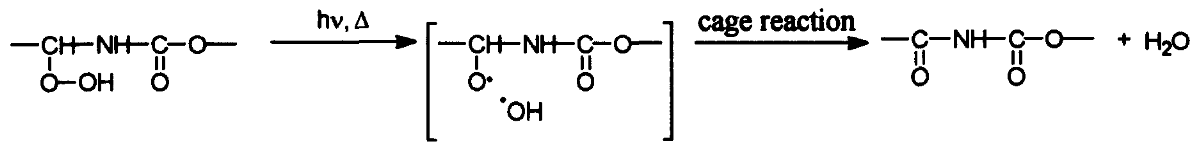

$$-\underset{\underset{O-OH}{|}}{CH}-NH-\underset{\underset{O}{\|}}{C}-O- \xrightarrow{h\nu,\Delta} \left[-\underset{\underset{O\bullet}{|}}{CH}-NH-\underset{\underset{O}{\|}}{C}-O- \quad {}^{\bullet}OH\right] \xrightarrow{\text{cage reaction}} -\underset{\underset{O}{\|}}{C}-NH-\underset{\underset{O}{\|}}{C}-O- + H_2O$$

This photoproduct corresponds to the absorption maximum at 1755 cm^{-1} (the corresponding model compound

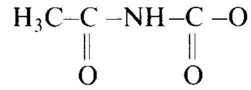

$$H_3C-\underset{\underset{O}{\|}}{C}-NH-\underset{\underset{O}{\|}}{C}-O-C_2H_5$$

gives two maxima at 1755 and 1700 cm^{-1}). However, as concerns the studied polyurethanes, no observation can be made around 1700 cm^{-1} since the decline of the urethane absorption bands prevents one from measuring absorption maxima that grow around this frequency. This photoproduct readily reacts with water formed *in situ* to give a carboxylic acid and a urethane group:

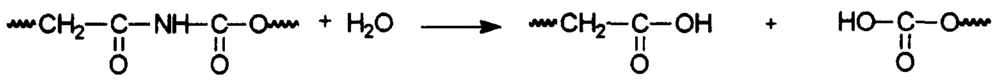

The formation of carboxylic acid accounts for the increase in the C=O band at 1715 cm^{-1}. The presence of carboxylic acid is also revealed by the reaction with SF_4 that leads to an acyl fluoride with a C=O band at 1841 cm^{-1}, and by the reaction with NH_3 that leads to the carboxylate salt with a $\nu(CO_2^-)$ band at 1560 cm^{-1}.

The formation of urethane end groups

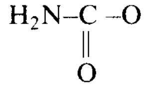

$$H_2N-\underset{\underset{O}{\|}}{C}-O$$

by conversion of in-chain urethane

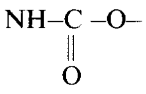

$$NH-\underset{\underset{O}{\|}}{C}-O-$$

is also evidenced from the comparison of the i.r. spectra of the photooxidized polymers with those of corresponding low molecular weight models (ethyl N-ethyl carbamate and ethyl carbamate). The amide II band at 1535 cm^{-1}, observed on the i.r. spectrum of ethyl N-ethyl carbamate, is missing on the i.r. spectrum of ethyl carbamate and replaced by an absorption band at 1605 cm^{-1}, δ (NH_2). A similar evolution has been reported for the photooxidized polymers (decrease of the band at 1540 cm^{-1} and growth of a band at 1607 cm^{-1}). In the domain of N–H stretching vibrations, the i.r. spectrum of ethyl carbamate shows three maxima (3471, 3355 and 3202 cm^{-1}) instead of one (3338 cm^{-1}) for ethyl N-ethyl carbamate. The decrease of the ν_{N-H} band (3320 cm^{-1}) and the presence of two of the three maxima were indeed observed on the i.r. spectra of the photooxidized polymers as reported above. Finally, as observed with the models, the ν_{C-N} vibration was shifted from 1040 cm^{-1} to 1071 cm^{-1}, and the initial amide III band at 1263 cm^{-1} decreased whereas three maxima at 1412, 1380 and 1334 cm^{-1} increased.

Radical III may also react by hydrogen abstraction and give an unstable hydroxylated product that is converted to an aldehyde group and a primary urethane. Aldehydes are readily oxidized in carboxylic acids[26]:

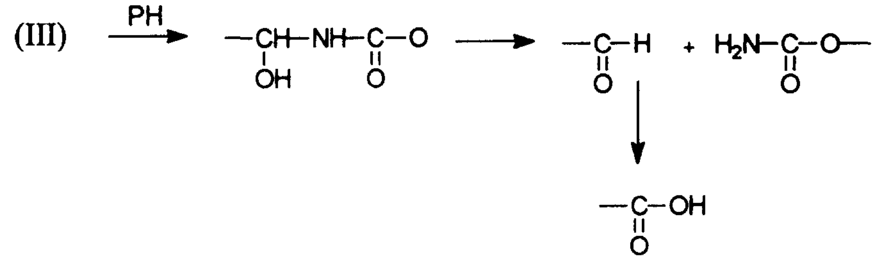

Acids can also be obtained by radical attack on hydroperoxide groups, as suggested in the following reaction reported in the case of polyethylene[27]:

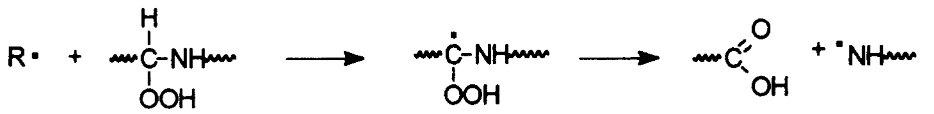

The products that are observed are similar to those obtained by hydrolysis of acetyl urethane groups.

A third way of evolution for radical III is a β-scission involving the homolysis of C–N bonds. The products formed by this reaction are indistinguishable from those reported above:

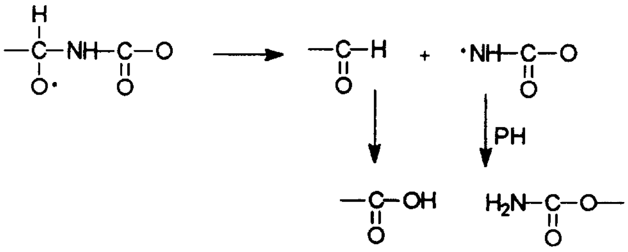

The last route of evolution of radical III is a β-scission involving the homolysis of C–C bonds:

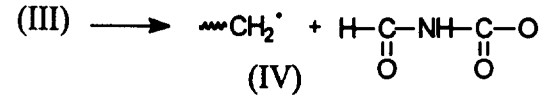

$$\text{(III)} \longrightarrow \sim\!CH_2^{\bullet} + \underset{\text{(IV)}}{H-\overset{}{\underset{\|\atop O}{C}}-NH-\underset{\|\atop O}{C}-O}$$

The alkyl end chain radical $CH_2\bullet$ reacts readily with oxygen to yield, by a classical chain oxidation scheme, several oxidation photoproducts including carboxylic acids (similar to those of the reaction above), peresters ($\bar{\nu}_{C=O} = 1785\,cm^{-1}$) and hydroxylated compounds (mainly alcohols) ($\bar{\nu}_{bonded\,OH} = 3450\,cm^{-1}$ and $\bar{\nu}_{C-O} = 1025\,cm^{-1}$). This is the only way to explain the product at $1785\,cm^{-1}$.

On irradiation at short wavelength ($\lambda = 254\,nm$), there is observed with HDI–BDO a loss of both types of methylene group in α position to the urethane groups

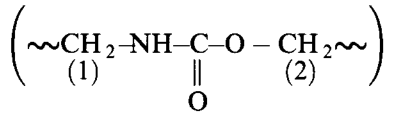

$$\left(\sim\!\underset{(1)}{CH_2}-NH-\underset{\|\atop O}{C}-O-\underset{(2)}{CH_2}\!\sim\right)$$

which indicates an oxidation of the carbon atoms in positions 1 and 2. Conversely, on irradiation at long wavelengths that leads to induced oxidation, there is observed only an oxidation of the methylene groups in α position to the NH of urethane groups (position 1). Since it is highly improbable that the oxidation site in a radical-induced oxidation is wavelength dependent, one has to suspect that the oxidation of the carbon atoms in position 2 involves at first a direct photoscission of the polymeric backbone. On irradiation at long wavelengths, this reaction is not observed to occur.

Three different scissions may be considered that explain why methylene absorbance decreases:

- Scission of the N–C bond as observed in the case of polyamides[28], leads to the formation of two radicals (V) and (VI):

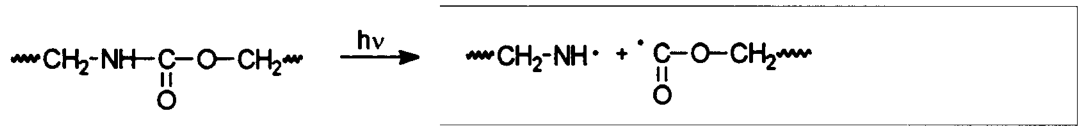

$$\sim\!CH_2-NH-\underset{\|\atop O}{C}-O-CH_2\!\sim \xrightarrow{h\nu} \sim\!CH_2-NH^{\bullet} + {}^{\bullet}\underset{\|\atop O}{C}-O-CH_2\!\sim$$

Radical (V) is the precursor of an amine whose formation contributes to the increase of absorbance at $1605\,cm^{-1}$. Radical (VI) evolves by loss of carbon dioxide, leading to an alkyl radical (VII):

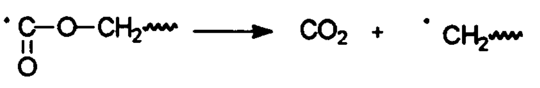

$${}^{\bullet}\underset{\|\atop O}{C}-O-CH_2\!\sim \longrightarrow CO_2 + {}^{\bullet}CH_2\!\sim$$

Oxidation of radical (VII) is responsible for the decrease of absorbance of methylene groups in α position to the

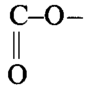

$$\underset{\|\atop O}{C}-O-$$

groups that is observed on irradiation at short wavelength.

Oxidation of radical (VII) leads to several photoproducts including, carboxylic acids and hydroxylated products. Oxidation of radical (VII) leads also to the formation of peresters, that may explain the absorption maximum at $1785\,cm^{-1}$.

- Scission of the O–C bond leads to radicals (VII) and (VIII):

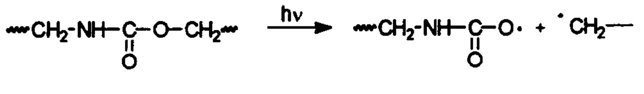

$$\sim\!CH_2-NH-\underset{\|\atop O}{C}-O-CH_2\!\sim \xrightarrow{h\nu} \sim\!CH_2-NH-\underset{\|\atop O}{C}-O^{\bullet} + {}^{\bullet}CH_2-$$

Radical (VIII) can decarboxylate and radical (V) is obtained:

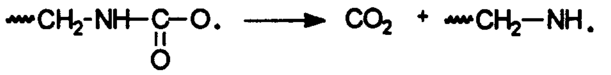

$$\sim\!CH_2-NH-\underset{\|\atop O}{C}-O^{\bullet} \longrightarrow CO_2 + \sim\!CH_2-NH^{\bullet}$$

- Scission of the C–N bond leads to radicals (VII) and (IX):

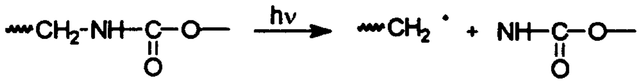

$$\sim\!CH_2-NH-\underset{\|\atop O}{C}-O- \xrightarrow{h\nu} \sim\!CH_2^{\bullet} + NH-\underset{\|\atop O}{C}-O-$$

Hydrogen abstraction by radical (IX) leads to a primary urethane.

It has been reported above that the proportion of hydroxylated compounds was higher on irradiation at short wavelength than at long wavelengths. This means that on irradiation at short wavelength those reactions that involve an initial photoscission of the C–N and O–C bonds are favoured in comparison to those involving an induced oxidation that leads mainly to the formation of acetylurethane groups.

In addition to the reaction of the urethane segments, short-wavelength irradiation provokes the decarboxylation of the polyester segments of ESHDI polymers. This reaction produces alkyl radical end groups that oxidize as in the reaction reported above:

$$\sim\!CH_2-O-CO-CH_2\!\sim \xrightarrow[h\nu]{\lambda = 254\,nm} \sim\!CH_2^{\bullet} + CO_2\uparrow + {}^{\bullet}CH_2\!\sim$$

CONCLUSION

The oxidation mechanism shown in *Scheme 3* can be proposed to explain the different routes of evolution of ESHDI polymers on irradiation at short or long wavelengths. This scheme prompts the following comments.

At $\lambda > 300\,\mathrm{nm}$, an induced oxzidation occurs, implying excitation of chromophoric defects. This reaction initiates oxidation of the methylene groups in α position to the NH of the urethane function. Neither induced oxidation of the methylene groups in α position to the

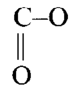

$$\overset{\displaystyle \mathrm{C{-}O}}{\underset{\displaystyle \mathrm{O}}{\|}}$$

of the urethane nor induced oxidation of the methylene groups of the soft polyester segments is observed to be an important path of evolution.

At $\lambda = 254\,\mathrm{nm}$, photoinitiation through direct excitation of the

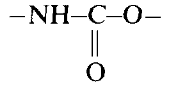

$$-\mathrm{NH}-\underset{\underset{\displaystyle \mathrm{O}}{\|}}{\mathrm{C}}-\mathrm{O}-$$

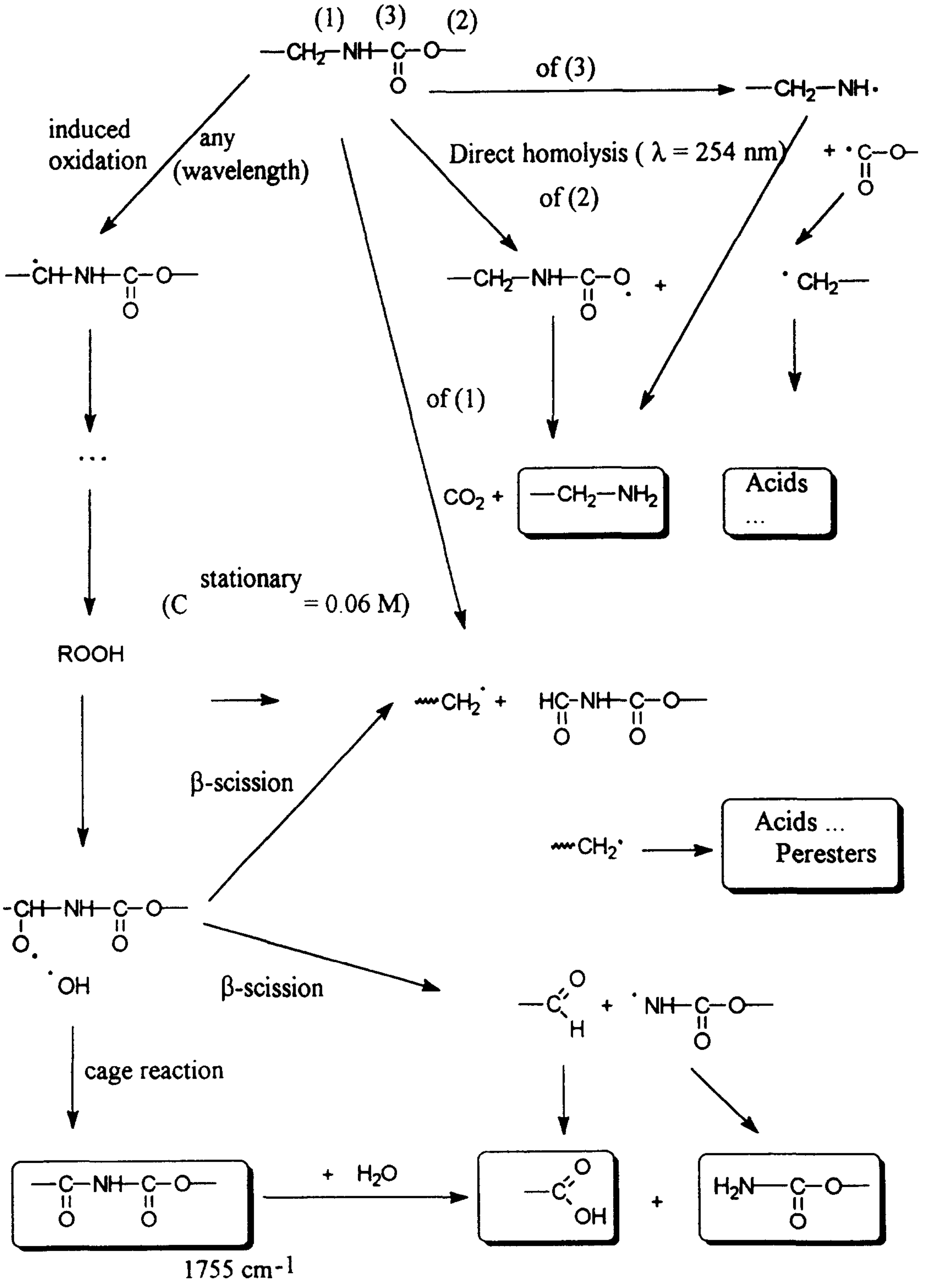

Scheme 3 Photooxidation mechanism for ESHDI polymers

chromophore occurs. Photoscission of C–N and O–C bonds is observed.

Scission of the O–C bond leads to the oxidation of the methylene groups in α position to the oxygen atom of the

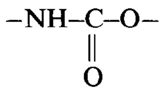

$-\mathrm{NH}-\underset{\underset{\mathrm{O}}{\|}}{\mathrm{C}}-\mathrm{O}-$

chromophore. At this irradiation wavelength, decarboxylation of the polyester segments through direct excitation of

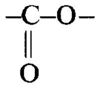

$-\underset{\underset{\mathrm{O}}{\|}}{\mathrm{C}}-\mathrm{O}-$

is observed.

ACKNOWLEDGEMENTS

The authors are deeply grateful to Pr Pascault and Dr Mechin for their help in making the polyurethane samples.

REFERENCES

1. Beachell, H. C. and Chang, I. L., *J. Polym. Sci., Part A1*, 1972, **10**, 503.
2. Schollenberg, C. S. and Stewart, F. D., in *Advances in Urethane Science and Technology*, Vol. 2, ed. K. C. Frisch and S. L. Reegen, Vol. 2. Technomic Publishing Co., Westport, CT, 1973, p. 71.
3. Schollenberger, C. S. and Stewart, F. D., in *Advances in Urethane Science and Technology*, Vol. 4, ed. K. C. Frisch and S. L. Reegen. Technomic Publishing Co., Westport, CT, 1976, p. 68.
4. Allen, N. S. and McKellar, J. F., *J. Appl. Polym. Sci.*, 1976, **20**, 1441.
5. Osawa, Z. and Nagashima, K., *Polym. Degrad. Stab.*, 1979, 311.
6. Brauman, S. K., Mayorga, G. D. and Hellen, J., *Ann. Biomed. Eng.*, 1981, **9**, 45.
7. Rek, V. and Bravar, M. J., *J. Elast. Plast.*, 1980, **12**, 245.
8. Gardette, J. L. and Lemaire, J., *Makromol. Chem.*, 1981, **182**, 2723.
9. Gardette, J. L. and Lemaire, J., *Makromol. Chem.*, 1982, **183**, 2415.
10. Hoyle, C. E. and Kim, K. J., *J. Polym. Sci., Polym. Chem. Ed.*, 1986, **24**, 1879.
11. Hoyle, C. E., Kim, K. J., No, Y. G. and Nelson, G. L., *J. Appl. Polym. Sci.*, 1987, **34**, 763.
12. Thapliyal, B. P. and Chandra, R., *Prog. Polym. Sci.*, 1990, **15**, 735.
13. Cuve, L. and Pascault, J. P., *Polymer*, 1991, **32**, 345.
14. Lemaire, J., Arnaud, R. and Gardette, J. L., *Rev. Gen. Caoutch. Plast.* 1981, **613**, 87.
15. Ly, Tang, Sallet, D. and Lemaire, J., *Macromolecules*, 1981, **15**, 1432.
16. Aldrich Library of Infrared Spectra, Edition III. Aldrich Chemical Co., Milwaukee, WI, 1981, p. 451.
17. Srichatrapimuk, V. W. and Cooper, S. L., *J. Macromol. Sci., Phys.*, 1978, **B15**(2), 267.
18. Avram, M. and Mateescu, G. D., *Spectroscopie Infrarouge*. Dunod, Paris, 1970, p. 547.
19. Seymour, R. W., Estes, G. M. and Cooper, S. L., *Polyurethane Elastomers*, 1970, (5), 579.
20. Coleman, M. N., Lee, K. H., Skrovanek, D. J. and Painter, P. C., *Macromolecules*, 1988, **19**, 2149.
21. Corish, P. J., *Anal. Chem.*, 1959, **37**, 1298.
22. Brunette, C. M., Hsu, S. L., Macknight, W. J. and Schneider, N. S., *Polym. Eng. Sci.*, 1981, **3**, 21.
23. March, J., *Advanced Organic Chemistry*. McGraw-Hill Kogakusha, Tokyo, 1977.
24. Carlsson, D. J., Brousseau, R., Zhang, C. and Wiles, D. M., *ACS Symp. Ser.*, 1988, **364**, 376.
25. Wilhelm, C. and Gardette, J.-L., *J. Appl. Polym. Sci.*, 1994, **51**, 1411.
26. Adams, J. H., *J. Polym. Sci., Part A1* 1970, **8**, 1077.
27. Lacoste, J. and Carlsson, D. J., *J. Polym. Sci., Part A, Polym. Chem.*, 1992, **30**, 493.
28. Roger, A., Sallet, D. and Lemaire, J., *Macromolecules*, 1985, **18**, 1771.